# PRELIMINARY STUDY OF CREEP THRESHOLDS AND THERMOMECHANICAL RESPONSE IN HAYNES 188 AT TEMPERATURES IN THE RANGE 649 TO 871 °C

J.R. Ellis, P.A. Bartolotta, and S.W. Mladsi*
NASA Lewis Research Center
Cleveland, Ohio

One effort within the HOST Program has been the development of an improved thermomechanical testing capability at the NASA Lewis Research Center. This work is part of a long-term research program aimed at developing advanced viscoplastic constitutive models for materials subjected to thermomechanical loadings (refs. 1, 2, and 3). As a result of this effort, two additional electrohydraulic test systems were recently installed in the Fatigue and Structures Laboratory. These systems incorporated a number of features intended to meet the special needs of high-precision deformation testing. Experience had shown that such experiments require optimum performance in the areas of servohydraulic response, specimen alignment, and specimen heating. The measures taken to assure such performance with the latest equipment are outlined in the first part of the paper.

The first series of experiments conducted on these test systems was in support of the Space Station Solar Receiver Program. By way of background, solar receivers, used in conjunction with compressors, turbines and generators, are intended to provide a continuous source of electrical power up to 25 kW per unit (fig. 1). One unique feature of the design shown is that it uses a phase change material (PCM) to store solar energy. Simply stated, the aim is to use the latent heat of solidification of the PCM as a source of thermal energy during periods of eclipse. The phase change material used is a LiF - $CaF_2$ eutectic which is stored in small canisters (1.78 in. o.d. x 1.0 in. long) manufactured from Haynes 188 (fig. 2). A total of 96 canisters are individually attached to each working fluid tube and the receiver is lined with 82 such tubes.

During review of the subject design, questions were raised regarding the validity of basing the design of the PCM containment canisters on purely elastic stress analysis. Two factors giving rise to this concern are the high operating temperatures, 694°C to 834°C, and the 30-year service life. The approach adopted in resolving these concerning was to determine the stress levels or "thresholds" at which creep deformations first become significant in Haynes 188 over the temperature range of interest. This was to be accomplished in a series of short-term creep tests conducted under constant stress and constant temperature. In service, however, solar receiver components experience thermal cycles at 1.5 hour intervals. A second series of experiments was conducted, therefore, to establish whether the thresholds determined under monotonic conditions also apply in the case of thermomechanical loading. The results obtained in the two series of experiments are described in the second part of the paper.

*Summer intern in the Case-NASA Cooperative Aerospace R&D Fellowship Program. Presently at Virginia Polytechnic Institute, Blacksburg, Virginia.

## EXPERIMENTAL DETAILS

An overall view of one of the closed-loop, electrohydraulic test systems is shown in Figure 3. The system features a two-post load frame with ±50 kip capacity. One point of interest is that the load cell is an integral part of the loadframe crosshead. This helps in keeping the length of the load train to a minimum which in turn helps in maintaining specimen stability under compressive loading. Another feature of the load frame is that it incorporates hydraulic bearings designed to impart high lateral stiffness to the linear actuator. Stiffness of this type is viewed as being a first requirement in achieving precise specimen alignment. With regards to servohydraulic response, the system incorporates dual 10 gpm servovalves. This particular combination was shown by trial to be capable of following rapid changes in programmed loading with high fidelity.

Further details of specimen gripping and specimen heating arrangements are shown in Figure 4. Specimens are installed in water-cooled hydraulic grips which incorporate collets for specimen gripping purposes. A variety of collets is available for testing flat plates, smooth shank cylindrical specimens, and threaded-end cylindrical specimens. Checkout experiments conducted using a number of strain gaged specimens clearly demonstrated the superiority of the smooth shank design in achieving minimum specimen bending. The results of checkout experiments obtained using such a specimen are shown for illustration purposes in Table 1. Here, it can be seen that careful grip alignment and use of smooth shank specimens resulted in specimen bending strains as low as $+10\mu\varepsilon$. note that in obtaining these results, the strain gages were zeroed before specimen installation and no further adjustments were made during the experiments. One interesting feature of these results is that the installation bending strains are not changed significantly by loading in either the tensile or the compressive senses. Further, the loading system can be seen to exhibit minimum hysteresis when the direction of loading is reversed.

Specimen heating is accomplished using 5 kW radio frequency (RF) induction heaters. One advantage of this approach is that it allows ready access to the specimen's surface. As indicated in Figure 4, this allows commercially available extensometers to be used for strain measurement with minimum complication. Further, RF heating can be used to advantage in thermomechanical tests because of the localized nature of specimen heating. This means that fairly rapid thermal cycling can be achieved, again with minimum complication. A major disadvantage of this heating method is that specimen temperature profiles are extremely sensitive to heater load coil design. Thus, considerable time can be spent with conventional coil designs in obtaining temperature profiles meeting ASTM requirements. This problem has been eliminated to a large extend by developing fixturing which allows load coils to be split into sections (fig. 4). Further, the fixturing allows individual sections to be adjusted in a straightforward and systematic manner in both the vertical and the radial senses. Recent experience has shown that this approach results in considerable time saving in obtaining optimum load coil configurations. Typical temperature profiles are shown in Table (2) for the experiments described in detail later in the paper. Inspection of these data shows that the ASTM requirement of being within ±1 percent of the mean temperature was met in all cases. It is re-emphasized that these results were obtained with minimum effort once the basic coil configuration had been decided.

Details of the thin-walled tubular specimen used in the investigation are given in Figure (5). The length of the parallel gage section is 1.375 inches, the o.d. is 0.450 inch, and the wall thickness is 0.060 inch. One less than desirable feature of the design is that it utilizes threaded ends. As indicated earlier, this compromises the excellent alignment possible with smooth shank designs. To illustrate, checkout experiments had shown that the use of threads can introduce installation bending strains as high as $\pm 300 \mu\varepsilon$ into a precisely aligned loading system. Unfortunately, the limited time available for this program meant that existing specimens had to be used and this in turn led to the use of the specimen design shown in Figure 5.

The material under investigation, Haynes 188, is a cobalt-based structural alloy. Two characteristics of the alloy important in the present application are good corrosion resistance and good high-temperature strength. The former property is obtained by including lanthanum in the alloy system which forms a protective oxide scale. High temperature strength is obtained by including tungsten which provides solid solution strengthening. Additional strengthening is provided by carbon which precipitates in the form of $M_6C$ and $M_{23}C_6$ carbides. The chemical composition specified for the alloy is compared in Table (3) to the results of analysis performed at NASA Lewis on the test material. The two most obvious deviations are that the percentage by weight of both tungsten and phosphorous fall above the specified range. Although these deviations might prove important in long-term service, they are not judged to be limiting in the present study.

## EXPERIMENTAL APPROACH

As noted earlier, the first objective of this work was to determine the stress levels or "thresholds" at which creep deformation becomes significant during the 1.5 hour hold periods typical of solar received service. As indicated in Figure 6, the approach adopted was to subject specimens to a series of short-term creep tests conducted under constant stress and constant temperature. The three temperatures selected for this stage of the program were 649, 760, and 871°C. The intent was to start at a low value of stress and to increase stress in a stepwise manner until some target value of creep strain was exceeded. Selection of this target value was not straightforward and involved a degree of judgment. Ideally, the value should be as small as possible to avoid changing the state of the material significantly during the course of the experiment. In practice, a combination of high and low frequency noise on the strain signals meant that a relatively large value of creep strain, ~ 50 $\mu\varepsilon$, was needed to avoid misinterpretation of the data. The high frequency noise, caused for the most part by the RF heating system, had a peak-to-peak value of about ±5 mV (± 10 $\mu\varepsilon$). The low frequency noise, resulting from cyclic variation of the laboratory environment, had a peak-to-peak value of about ±10 mV (±20 $\mu\varepsilon$). With these values in mind, a target value of ~ 50 $\mu\varepsilon$ appeared to be a reasonable compromise.

Because of the uncertainties noted above, two experiments were judged to be necessary to establish thresholds at a particular temperature. The first was viewed as being exploratory and the second as being an attempt to determine a more precise value. It should be noted that a fresh specimen was used in each experiment. Adopting this approach, the specimen used in the second experiment had not experienced prior inelastic straining. Stated differently, the final threshold determination was made on material in the original solution annealed condition. The initial stress values and stress increments used in these

experiments are summarized in Table (4). As indicated, relatively large stress increments were used in the first experiment to establish the approximate location of the threshold with a minimum of loading steps. These experiments showed that the thresholds fall within the following stress ranges: 30 to 35 ksi at 649°C, 5 to 11 ksi at 760°C, and 2 to 4 ksi at 871°C. In light of this information, more realistic initial stresses could be selected for the second experiment. This in turn meant that that stress increments could be kept as small as possible. As indicated in Table (4), a value of 1 ksi was used in final threshold determinations at all three temperatures.

Selection of the test values for the thermomechanical experiments was more straightforward. This was because the results of thermal analysis and elastic stress analysis were available to help guide this process. With regard to temperature values, analysis had shown that the peak solar flux occurs at an axial location about 3 feet from the aperture plate (fig. 1). A thermal history for a canister at this location is shown in idealized form in Figure 7. On coming out of eclipse, time zero in the figure, the PCM is in solid form and the canister temperature is 649°C at the location selected for detailed analysis. During the first 10 minutes, temperature increases to a value of 778°C at which point the PCM starts to liquify. The peak temperature of the cycle, 834°C, is reached after about 52 minutes, at which time the space station goes into eclipse. Subsequently, the canister temperature drops quite rapidly to a value of about 778°C when the PCM starts to solidify. Temperature then remains constant until the solidification process is completed at about 80 minutes into the cycle. During the balance of the cycle, heat is rejected from the receiver with the PCM in solid form. After about 90 minutes, the space station comes out of eclipse and the cycle is repeated. The combinations of temperature and time used in simulating this cycle under computer control are summarized in Table (5). As indicated in the table, a single temperature history was used throughout.

As noted earlier, an elastic stress analysis had been performed using the MARC finite element code. The aim of this analysis had been to determine the maximum values of stress and strain introduced into canisters by the thermal cycle described above. The stresses determined in this analysis are listed in Table (5) under the heading, Test 1. As implied by this designation, the first test was an attempt to simulate service conditions as predicted by preliminary analysis. It can be seen that the maximum and minimum stresses predicted for service are 7.21 ksi and 3.22 ksi and that the mean stress is about 5.16 ksi. Because of concerns regarding electrical noise, it was decided to conduct two additional experiments at somewhat higher stresses. This was accomplished by simply conducting the additional tests at higher values of mean stress. As indicated in Table (5), the mean stresses for Tests 2 and 3 were 6.17 ksi and 10.16 ksi. In summary, the approach adopted in conducting thermomechanical tests was to use computer control to subject specimens to predetermined temperature cycles and stress cycles. It was anticipated at any inelastic deformation occurring in the material would be detected by the mechanical extensometer used to monitor strain. This particular mode of control was adopted for reason of experimental convenience.

## EXPERIMENTAL RESULTS

The data obtained in the threshold experiments conducted at 871°C are shown for illustration purposes in Figures 8 and 9. Data was acquired in these experiments using strip chart recorders. This was the preferred method since

recordings made in this manner provided a clear indication of both the high frequency and the low frequency noise. Average curves were fitted by hand to establish the amount of creep strain, $\varepsilon_c$, accumulated during the 1.5 hour hold periods. An assessment was then made regarding the stress level giving the target value of creep strain. Creep thresholds determined in this manner are summarized in Table (6) for the three temperatures investigated.

Strip chart records were also used in the thermomechanical experiments because of noise considerations. In these experiments, recordings were made of temperature versus time, stress versus time, and total strain versus time. Temperature and stress were monitored to check how closely the programmed waveforms were being followed. As no control problems were encountered in these experiments, the recordings were near-identical to those programmed.

The data of primary interest in these experiments were the recordings of total strain versus time. To aid the reduction process, these recordings were digitized and all subsequent reduction performed using a personal computer. A plot of total strain versus time regenerated using the computer is shown in Figure 10. As indicated, the digitized data represents average behavior for the major part of the cycle. An attempt was made, however, to represent the raw data as closely as possible for times ranging from 10.5 minutes to 51.5 minutes. This was because almost all the inelastic straining had been found to occur during this portion of the cycle.

Raw data were also recorded during the thermomechanical tests on x-y plotters. Following normal practice, stress was recorded as ordinate and total strain as abscissa. Stress-strain hysteresis loops determined in this manner are shown in Figures 11 and 12 for cycles 1 and 5 of the thermomechanical test with a mean stress of 10.16 ksi. Originally, data in this form were intended to fulfill a backup role. In the event, hysteresis loops of this type were found to be useful in establishing average slopes relating stress and total strain for portions of the cycle involving purely elastic response. These values were used to check the accuracy of computer generated data.

One feature of the data described thus far is that the total strain includes a component resulting from thermal expansion of the specimen. An experimental approach was used to establish this apparent strain. Prior to thermomechanical testing, specimens were subjected to thermal cycles with the stress held at zero. The output of the extensometer in these experiments provided a direct measure of the apparent strain. It was then assumed that this apparent strain versus time history also applied under thermomechanical loading conditions. Adopting this approach, it was possible to subtract the apparent strain from the total strain during a cycle and to determine the corresponding values of mechanical strain. Plots of stress versus mechanical strain could then be determine, as illustrated in Figures 13 and 14. It should be noted that determination of data in this form was not straightforward because the mechanical component of strain frequently was small compared to the apparent component. This meant that any errors in the experimental determination of apparent strain caused large errors in the computed values of mechanical strain.

The data reduction process was carried one stage further by calculating the time dependent strains. As noted earlier, essentially all inelastic straining occurred during the portion of cycles corresponding to time ranging from 10.5 minutes to 51.5 minutes. The time dependent component of strain was

obtained for this portion of loading by subtracting the elastic components from the mechanical component. The values of Young modulus used in these calculations were obtained from the initial loading stage of the threshold experiments. Creep curves determined in this manner are shown in Figure 15 and 16. Note that time zero in these plots corresponds to 10.5 minutes into the thermomechanical cycle.

## DISCUSSION

Consideration is given first to the performance of the electrohydraulic test system used in this investigation. As noted earlier, the three areas of particular interest are servohydraulic response, specimen alignment, and specimen heating. The results shown in Tables (1) and (2) clearly indicated that very precise specimen alignment and temperature profiles are attainable with the subject test system. Whether or not improved servohydraulic response is possible with these systems remains to be demonstrated. However, the electrical noise problems arising in the threshold experiments indicated that further improvements are necessary in the area of specimen heating. The possibility of using solid state RF generators which generate minimum noise presently is being investigated.

The results shown in Figures 8 and 9 were taken to indicate that creep thresholds can be determined using the latest electrohydraulic test equipment, provided test durations are relatively short and relatively large accumulations of creep strain are used in defining the threshold. Significant improvements in specimen heating and in the control of laboratory environment are necessary if these conditions are to be relaxed. Another concern in these threshold determinations is that the practice of conducting a series of loadings on a single specimen is open to question. The concern here is that these loadings can alter the state of the material. Evidence of this can be seen in Figure 9 where the test conducted at 5.13 ksi resulted in 74 $\mu\varepsilon$ of creep strain being accumulated during the 1.5 hour hold period. It appears likely that this relatively low value resulted from the material being "hardened" as a result of the two prior loadings. The obvious solution to the problem is to use a number of fresh specimens in identifying the threshold condition. However, such an approach might prove time consuming, particularly if the data exhibit significant scatter.

As shown in Table (6), the threshold experiments showed the expected result that early creep response is highly temperature dependent. It can be seen that at 649°C, stress levels must exceed 30 ksi before creep strains become significant during the 1.5 hour hold periods. At temperatures of 760°C and 871°C, the corresponding values of stress are 11 ksi and 4 ksi, respectively. One important point to be noted about this result is that it would not have been predicted by inspection of handbook data. This is because material handbooks provide little or no information regarding the early stages of creep. It follows that problems can arise if decisions regarding the need for inelastic analysis are based on casual inspection of handbook data. The present study clearly indicated that some form of inelastic analysis is necessary for components operating at temperatures as high as 871°C if stress levels are expected to exceed 4 ksi.

Turning to the results of the thermomechanical experiments, no difficulties were experienced in simulating the anticipated service history of the solar receiver canisters. Problems did arise, however, in interpreting the data

generated at the lower stress levels because of the electrical noise problems discussed earlier. For this reason, attention will be directed first at the results obtained for the cycle involving a 10.16 mean stress. The most obvious feature of the data shown in Figure 13 is that it exhibits creep ratchetting. That is creep strains are accumulated on a cycle-by-cycle basis resulting in large overall accumulations of strain in relatively few cycles. For the data shown in Figure 13, almost 0.1 percent strain was accumulated in five cycles. Clearly, ratchetting of this type should be given serious consideration in design applications involving service lives of the order of 30 years.

Another feature of the data shown in Figure 13 is that the amount of creep strain accumulated per cycle decreases as the number of cycles is increased. On Cycle (1), for example, the accumulated creep strain is ~ 100 $\mu\varepsilon$. One interpretation of this result is that the material is hardening and might shake down to purely elastic response given a sufficient number of cycles. It should be noted, however, that shutdown and subsequent startup of the solar received could reinitiate the ratchetting process.

Similar ratchetting behavior can be observed in the data shown in Figure 14 for a mean stress 6.17 ksi. In this case, the creep strain accumulated during cycle (1) was about 100 $\mu\varepsilon$. On subsequent cycles, the creep occurring per cycle was ~ 50 $\mu\varepsilon$ or less and the data exhibited considerable scatter. The reason for the scatter is the electrical noise which complicated interpretation of the 6.17 ksi mean stress data. As might be expected, the situation was even worse for the 5.16 ksi mean stress data, the noise preventing meaningful analysis of the data.

Finally, attention is directed at the creep curves shown in figures 15 and 16. The somewhat unusual form of these curves is due, of course, to the fact that both temperature and stress are varying during the test. It was found that the curves could be fitted quite closely using second order polynomials. No physical significance is attached to this result, the expressions being reported to aid regeneration of the data. The results shown in Figure 16 can be seen to exhibit considerable scatter. It can also be seen that the results obtained for cycles (2) and (5) are not shown. This was because these creep curves exhibited excessive scatter and were not thought to be meaningful. Unfortunately, this was also the case for the creep curves determined for a mean stress of 5.16 ksi. Regardless of these data reduction difficulties, the observation was that considerable inelastic straining occurred in all three thermomechanical experiments.

## CONCLUSIONS

The following conclusions were drawn from this preliminary study of creep thresholds and thermomechanical response in Haynes 188:

1. Creep threshold can be determined using the latest electrohydraulic test equipment, provided test durations are short and relatively large accumulations of creep strain are used in defining the threshold.

2. Significant creep strains were measured under monotonic loading as stress levels as low as 4 ksi at temperatures predicted for solar receiver service.

3. The material exhibited creep ratchetting during simulated service cycles. This result was not predicted by analysis using current constitutive models for Haynes 188.

## FUTURE WORK

An experimental program will be initiated to develop an advanced viscoplastic constitutive model for Haynes 188. The model will be implemented in a general purpose finite element code and the analysis of critical components repeated. Further, steps will be taken to include Haynes 188 in existing research programs aimed at developing improved damaging modeling techniques for applications involving extended service at elevated temperatures.

## REFERENCES


1. Robinson, D. N. and Bartolotta, P. A.: Viscoplastic Constitutive Relationships with Dependence on Thermomechanical History. NASA CR-174836 (University of Akron), March 1985.

2. Bartolotta, P. A.: Thermomechanical Cyclic Hardening Behavior of Hastelloy-X. NASA CR-174999 (University of Akron), November 1985.

3. Ellis, J. R., Bartolotta, P. A., Allen, G. P., and Robinson, D. N.: Thermomechanical Characterization of Hastelloy-X under Uniaxial Cyclic Loading. NASA CP 2444, October 1986.


| LOAD (lb) | STRAIN AT LOCATION INDICATED (με) | | | | AVERAGE STRAIN (με) | BENDING STRAIN AT LOCATION INDICATED (με) | | | |
|---|---|---|---|---|---|---|---|---|---|
| | 1 | 2 | 3 | 4 | | 1 | 2 | 3 | 4 |
| 0 | -9 | 5 | 8 | -5 | -1 | -8 | 6 | 9 | -4 |
| 1000 | 162 | 175 | 177 | 166 | 170 | -8 | 5 | 7 | -4 |
| 2000 | 330 | 345 | 346 | 335 | 339 | -9 | 6 | 7 | -4 |
| 3000 | 449 | 514 | 515 | 504 | 508 | -9 | 6 | 7 | -4 |
| 2000 | 330 | 345 | 346 | 334 | 339 | -9 | 6 | 7 | -5 |
| 1000 | 161 | 176 | 178 | 165 | 170 | -9 | 6 | 8 | -5 |
| 0 | -9 | 7 | 8 | -6 | 0 | -9 | 7 | 8 | -6 |
| -1000 | -179 | -164 | -162 | -177 | -171 | -8 | 7 | 9 | -6 |
| -2000 | -347 | -332 | -331 | -346 | -339 | -8 | 7 | 8 | -7 |
| -3000 | -515 | -500 | -499 | -514 | -507 | -8 | 7 | 8 | -7 |
| -2000 | -347 | -331 | -330 | -345 | -338 | -9 | 7 | 8 | -7 |
| -1000 | -179 | -163 | -162 | -178 | -171 | -8 | 8 | 9 | -7 |
| 0 | -8 | 7 | 8 | -7 | 0 | -8 | 7 | 8 | -7 |

NOTE: THE STRAIN GAGES WERE LOCATED AT 90° INTERVALS AT THE SPECIMEN'S MIDSECTION. NUMBERING WAS IN THE COUNTERCLOCKWISE SENSE, VIEWED FROM ABOVE, AND LOCATION 1 CORRESPONDS TO THE FRONT OF THE TEST SYSTEM.

TABLE (1) SPECIMEN BENDING AFTER LOAD TRAIN ALIGNMENT

| THERMO-COUPLE NUMBER | THERMOCOUPLE LOCATION | NOMINAL TEST TEMPERATURE (°C) | | | | | | | |
|---|---|---|---|---|---|---|---|---|---|
| | | 647 | | 760 | | 871 | | 778 | |
| | | TEST 1 | TEST 2 | TEST 3 | TEST 4 | TEST 5 | TEST 6 | TEST 7 | TEST 8 |
| 1 | 0.25 in. ABOVE MIDSECTION | 644 | 640 | 758 | 757 | 874 | 870 | 774 | 773 |
| 2 | 0.25 in. ABOVE MIDSECTION | 643 | 645 | 757 | 756 | 867 | 868 | 773 | 770 |
| 3 | AT MIDSECTION | 646 | 649 | 757 | 759 | -- | 866 | 781 | -- |
| 4 | AT MIDSECTION | 645 | 648 | 761 | 760 | 877 | 870 | 777 | 773 |
| 5 | 0.25 in. BELOW MIDSECTION | 649 | 643 | 757 | -- | 879 | 877 | 780 | 773 |
| 6 | 0.25 in. BELOW MIDSECTION | 645 | 650 | 757 | 759 | 879 | 877 | 778 | 773 |

NOTE: THERMOCOUPLES AT PARTICULAR SPECIMEN LOCATIONS ARE DIAMETRICALLY OPPOSED. FURTHER, THERMOCOUPLES 1, 3, AND 5 ARE ALIGNED WITH THE SPECIMEN AXIS, AS ARE THERMOCOUPLES 2, 4, AND 6.

TABLE (2) - TEMPERATURE PROFILES OVER 0.5 in. SPECIMEN GAGE LENGTHS

| ELEMENT (Wt %) | | | | | | | | | | | |
|---|---|---|---|---|---|---|---|---|---|---|---|
| Co | Cr | Ni | W | Fe | Mn | Si | C | La | B | P | S |
| SPECIFIED CHEMICAL COMPOSITION | | | | | | | | | | | |
| BAL. | 21 to 23 | 20 to 24 | 13 to 15 | 3 max. | 1.25 max. | 0.2 to 0.5 | 0.05 to 0.15 | 0.03 to 0.12 | 0.05 max. | 0.02 max. | 0.015 max. |
| MEASURED CHEMICAL COMPOSITION | | | | | | | | | | | |
| 34.2 | 21.0 | 23.6 | 17.5 | 1.5 | 0.8 | 0.4 | 0.14 | 600 (ppm) | 400 (ppm) | 0.6 | 0.001 |

TABLE (3)-COMPARISON OF SPECIFIED AND MEASURED CHEMICAL COMPOSITIONS FOR HAYNES 188

| TEMPERATURE (°C) | TEST 1 | | TEST 2 | |
|---|---|---|---|---|
| | INITIAL STRESS (ksi) | STRESS INCREMENT (ksi) | INITIAL STRESS* (ksi) | STRESS INCREMENT (ksi) |
| 649 | 5 | 5 | 30 | 1 |
| 760 | 5 | 5 | 6 | 1 |
| 871 | 2 | 2 | 2 | 1 |

*VALUES BASED ON THE RESULTS OF THE FIRST EXPERIMENT

TABLE (4) -- SUMMARY OF STRESS LEVELS USED IN ESTABLISHING CREEP THRESHOLDS

| TIME (MIN.) | TEMPERATURE AND STRESS VALUES | | | |
|---|---|---|---|---|
| | TEMPERATURE (°C) | STRESS (ksi) TEST (1) | TEST (2) | (TEST 3) |
| 0 | 694 | 3.22 | 4.22 | 8.23 |
| 10.5 | 778 | 5.16 | 6.17 | 10.16 |
| 51.5 | 834 | 7.21 | 8.25 | 12.23 |
| 57.0 | 778 | 5.32 | 6.33 | 10.33 |
| 79.7 | 778 | 4.93 | 5.91 | 9.91 |
| 91.0 | 694 | 3.22 | 4.22 | 8.23 |

TABLE (5) -- COMBINATIONS OF TEMPERATURE AND STRESS USED IN DEVELOPING IDEALIZED THERMOMECHANICAL CYCLES

| TEMPERATURE (°C) | CREEP THRESHOLD* (ksi) |
|---|---|
| 649 | 30 |
| 760 | 11 |
| 871 | 4 |

*STRESS LEVELS AT WHICH CREEP STRAINS ~ 50$\mu\epsilon$ WERE ACCUMULATED DURING 90 MINUTE PERIODS

TABLE (6) -- CREEP THRESHOLDS DETERMINED FOR HAYNES 188 AT TEMPERATURES IN THE RANGE 649°C TO 871°C

# DESIGN CONCEPT FOR SPACE STATION SOLAR RECEIVER

DIAMETER, 6.1 FT; LENGTH, 9.8 FT

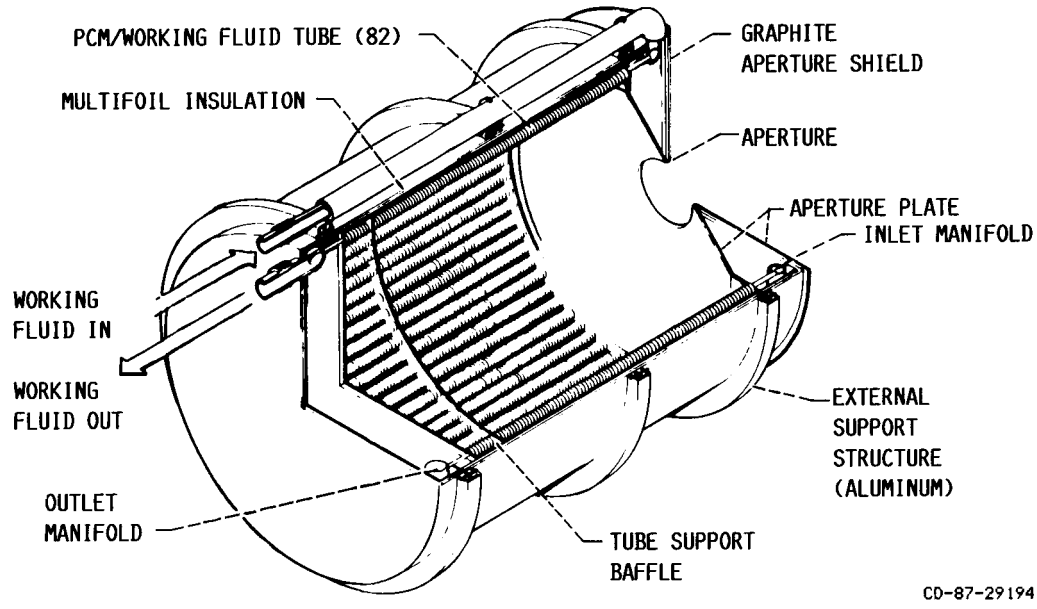


Figure 1

# POSSIBLE SOLAR RECEIVER TUBE CONFIGURATION

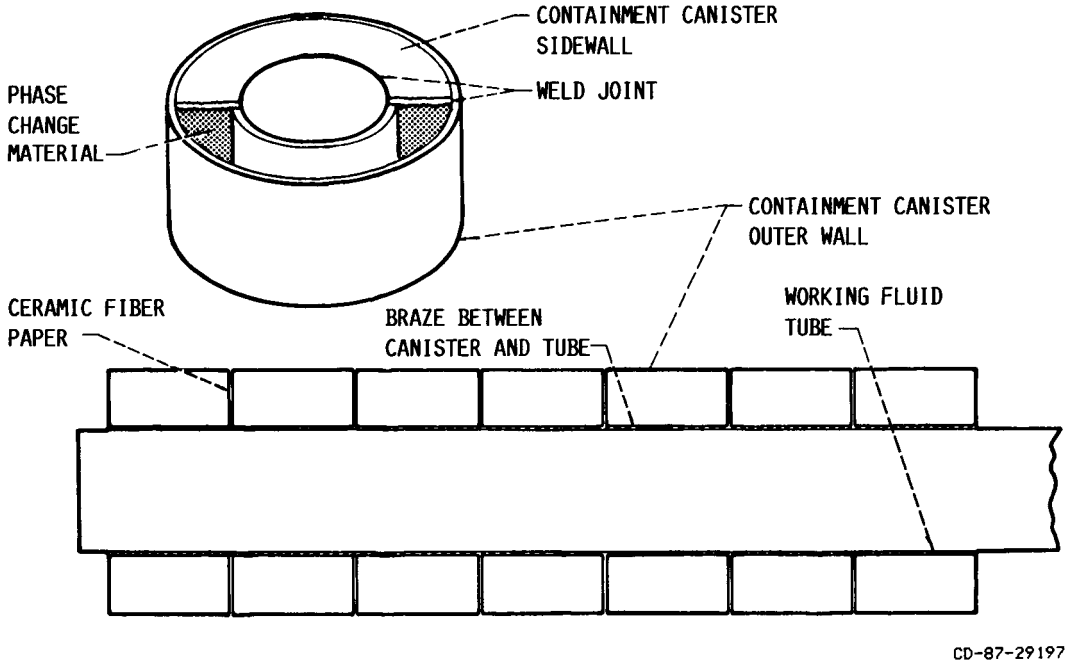


Figure 2

## OVERALL VIEW OF THE CLOSED LOOP, ELECTROHYDRAULIC TEST SYSTEM


CD-87-29200

Figure 3

## METHOD OF SPECIMEN HEATING AND STRAIN MEASUREMENT


CD-87-29199

Figure 4

# DETAILS OF THE THIN-WALLED TUBULAR SPECIMEN

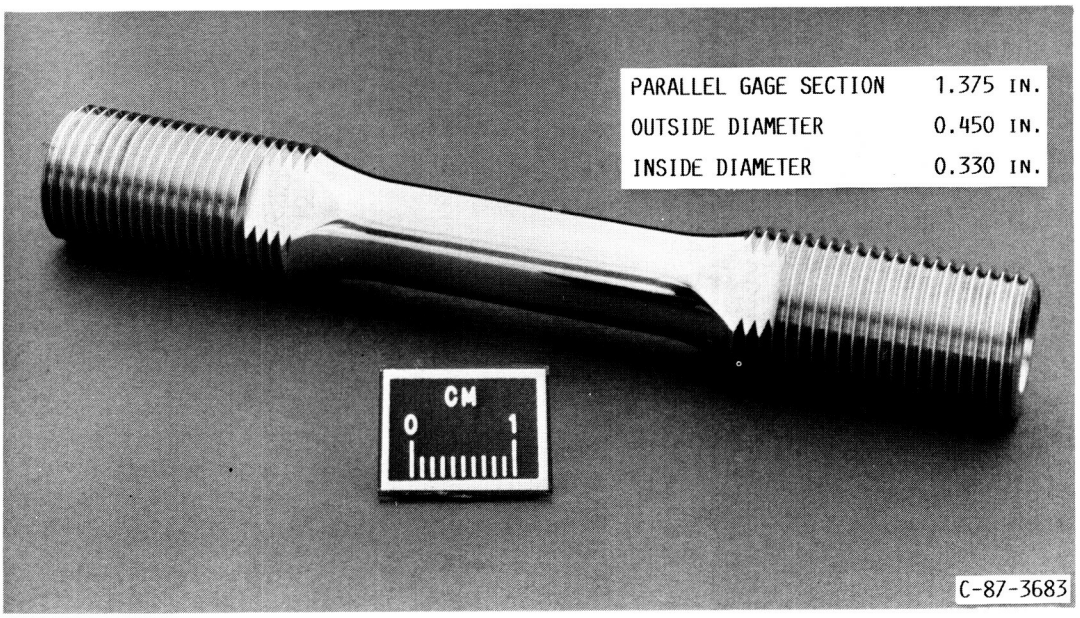


CD-87-29198

Figure 5

# APPROACH ADOPTED IN DETERMINING CREEP THRESHOLDS UNDER ISOTHERMAL CONDITIONS

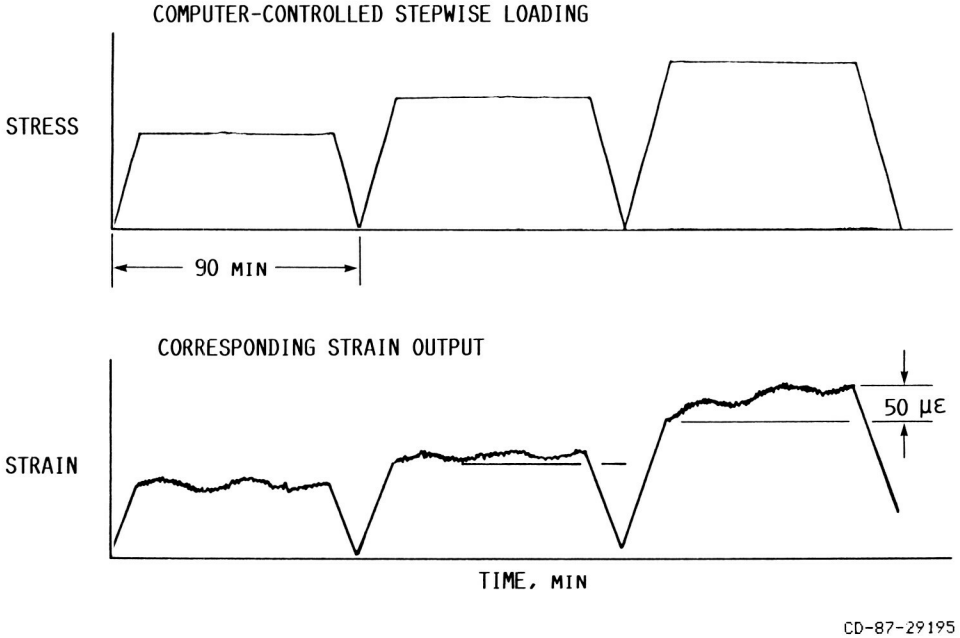


CD-87-29195

Figure 6

# THERMOMECHANICAL CYCLE FOR MEAN STRESS LEVEL OF 10.16 ksi

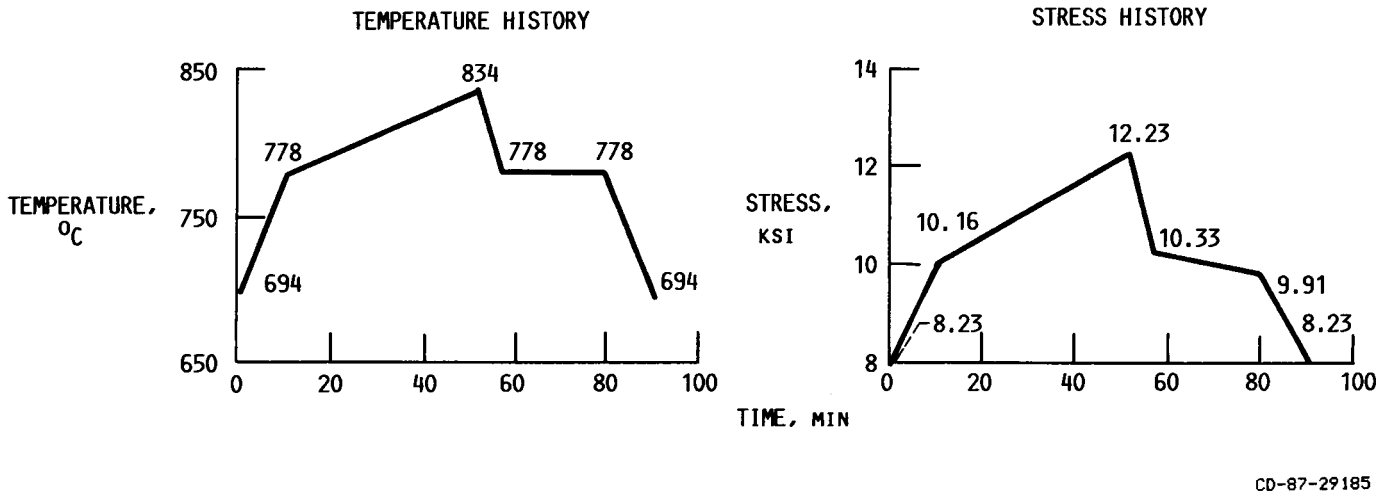


Figure 7

# SHORT-TERM CREEP RESPONSE OF HAYNES-188 DETERMINED UNDER THREE LEVELS OF LOADING AT 871 °C

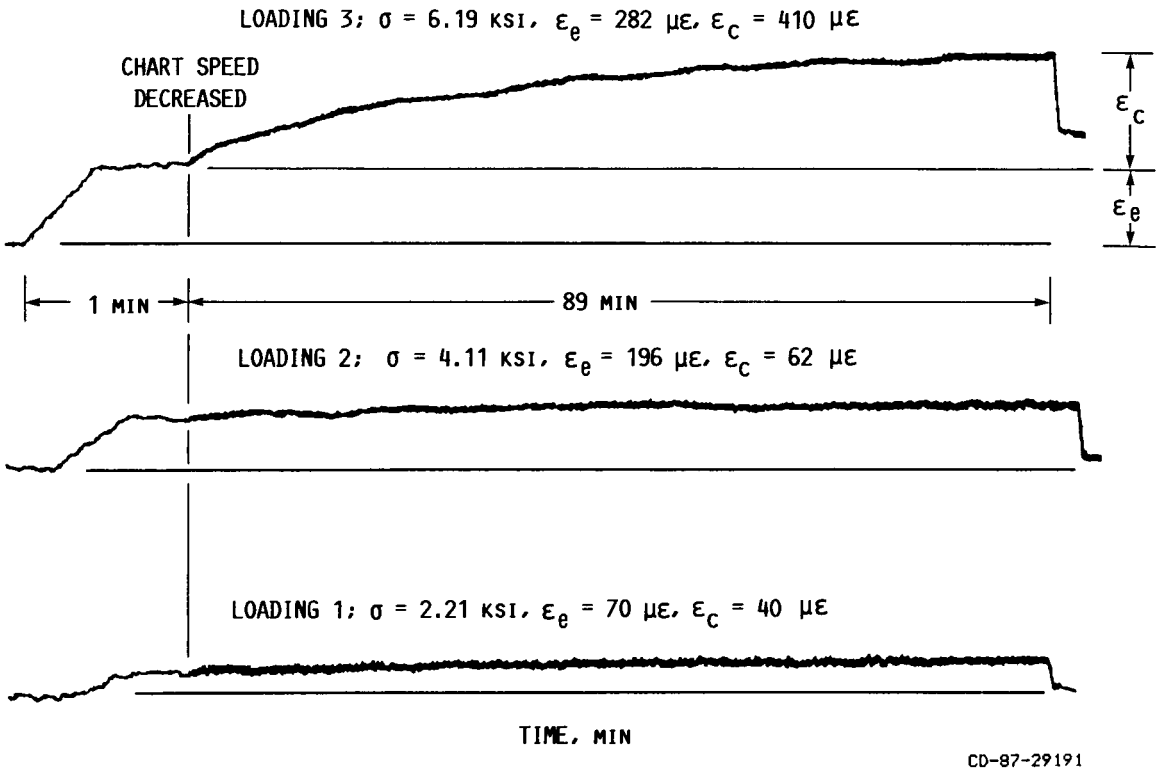


Figure 8

## SHORT-TERM CREEP RESPONSE OF HAYNES-188 DETERMINED UNDER FOUR LEVELS OF LOADING AT 871 °C

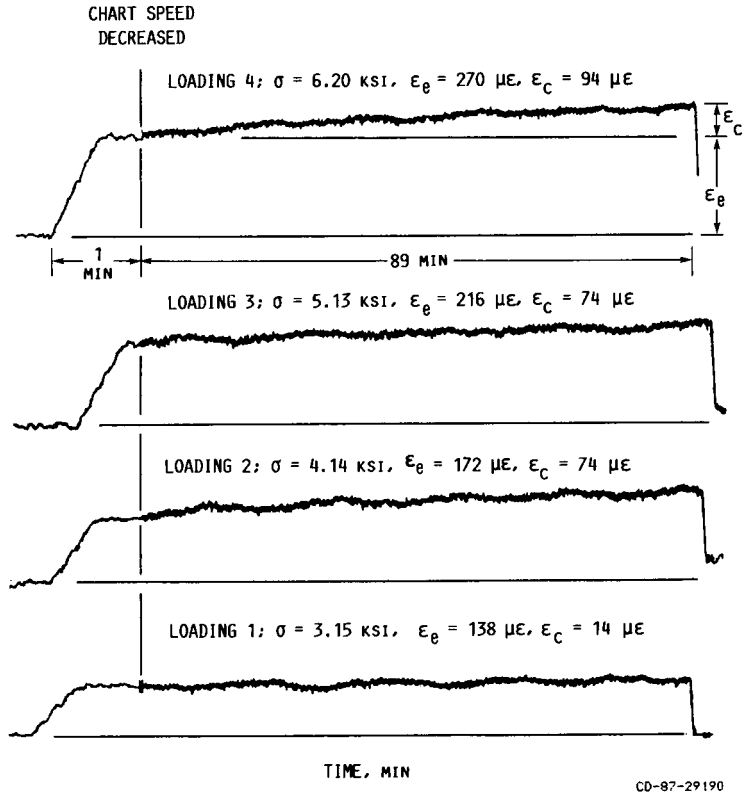


Figure 9

## TOTAL STRAIN VERSUS TIME HISTORY OBTAINED UNDER THERMOMECHANICAL LOADING FOR CYCLE 1

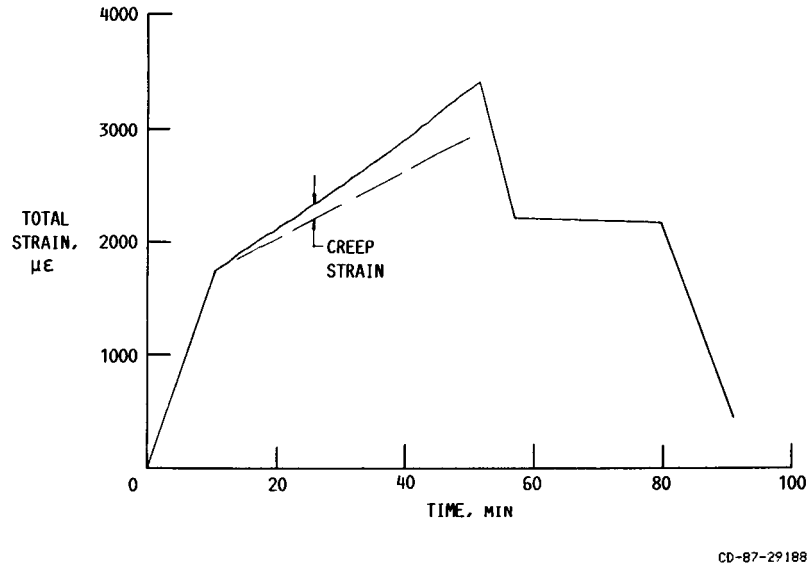


Figure 10

## STRESS-STRAIN RESPONSE OBTAINED UNDER THERMOMECHANICAL LOADING FOR CYCLE 1

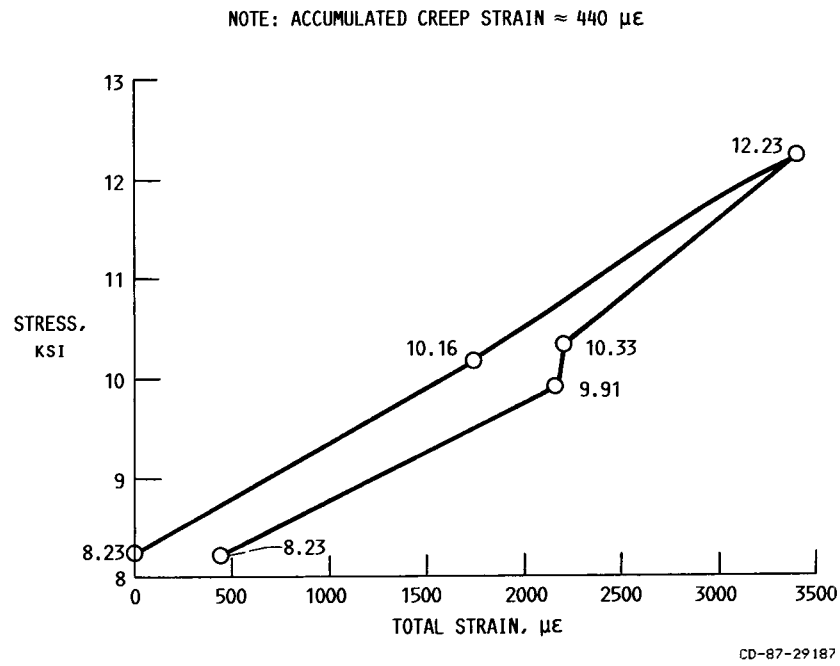


Figure 11

## STRESS-STRAIN RESPONSE OBTAINED UNDER THERMOMECHANICAL LOADING FOR CYCLE 5

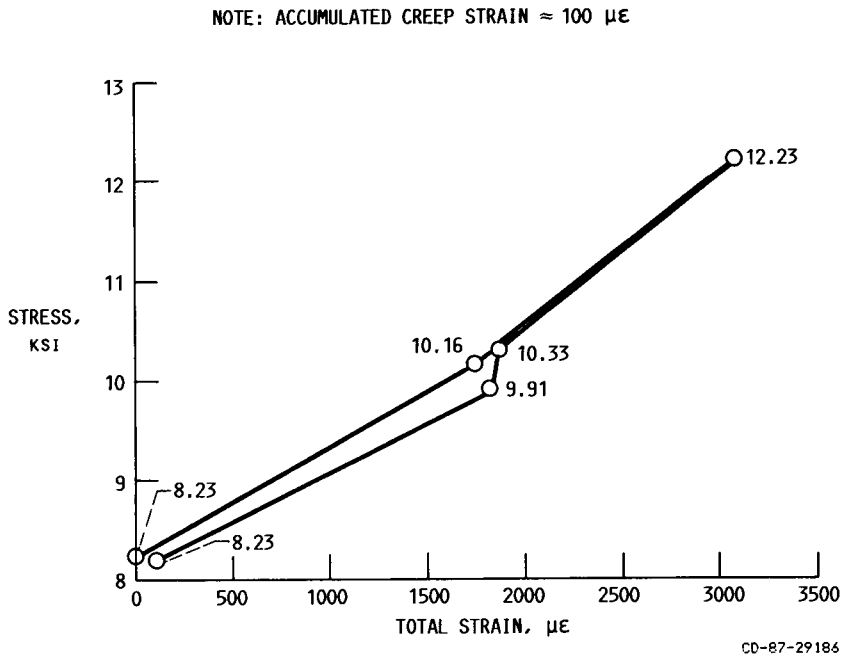


Figure 12

## CREEP RATCHETTING RESULTING FROM THERMOMECHANICAL CYCLES FOR 10.16-ksi MEAN STRESS

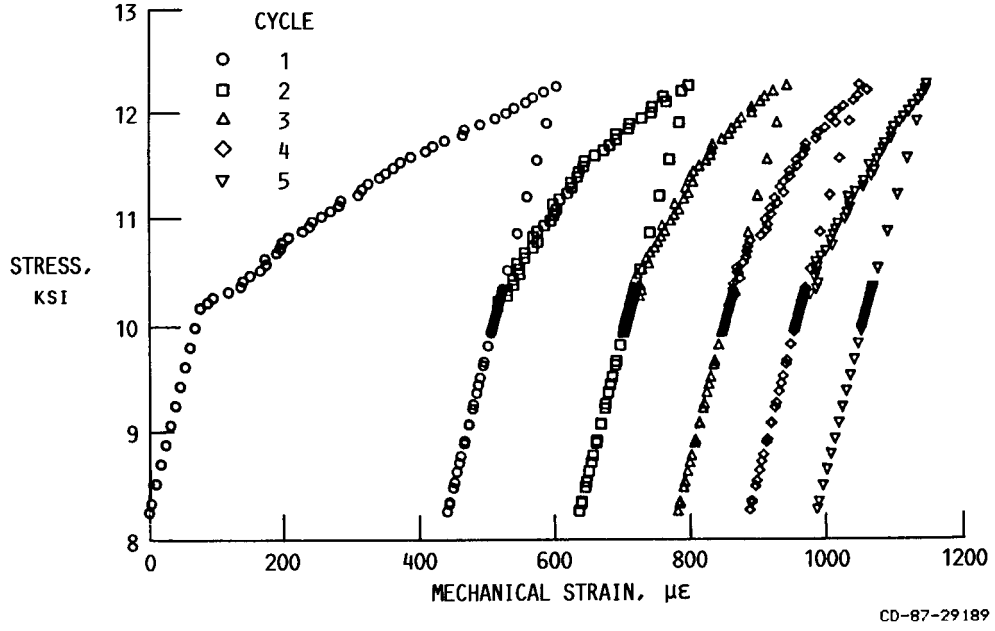


Figure 13

## CREEP RATCHETTING RESULTING FROM THERMOMECHANICAL CYCLING FOR 6.17-ksi MEAN STRESS

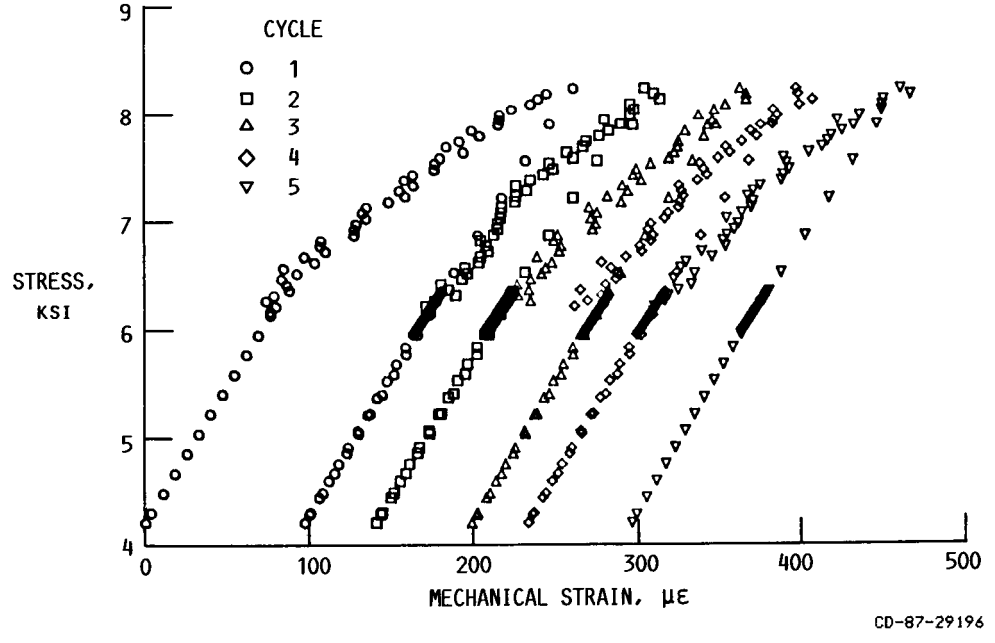


Figure 14

## CREEP RESPONSE UNDER THERMOMECHANICAL LOADING FOR 10.16-ksi MEAN STRESS

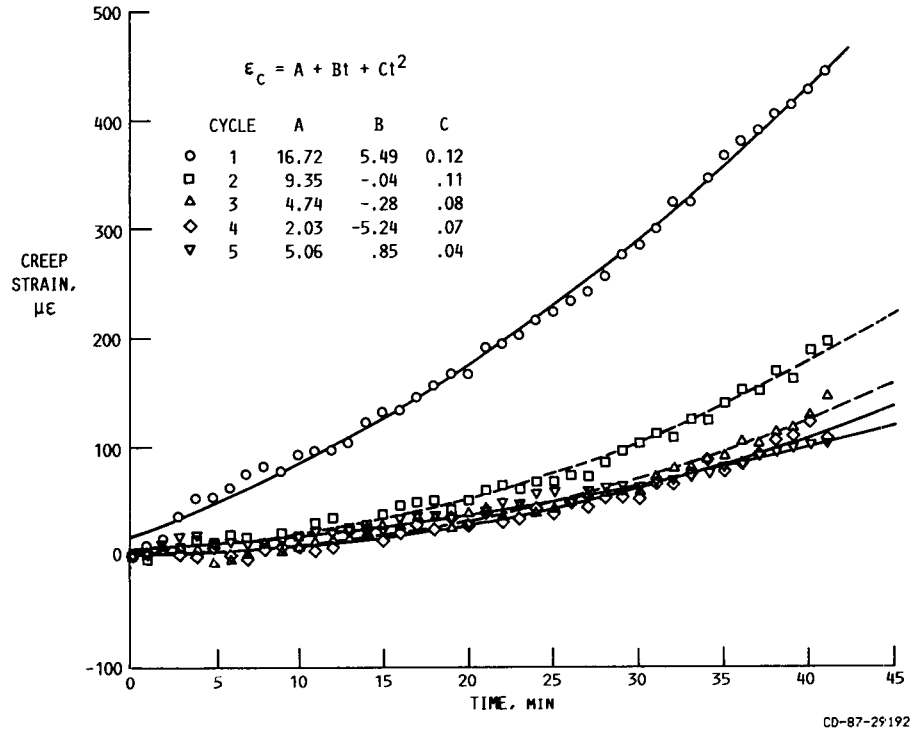


Figure 15

## CREEP RESPONSE UNDER THERMOMECHANICAL LOADING FOR 6.17-ksi MEAN STRESS

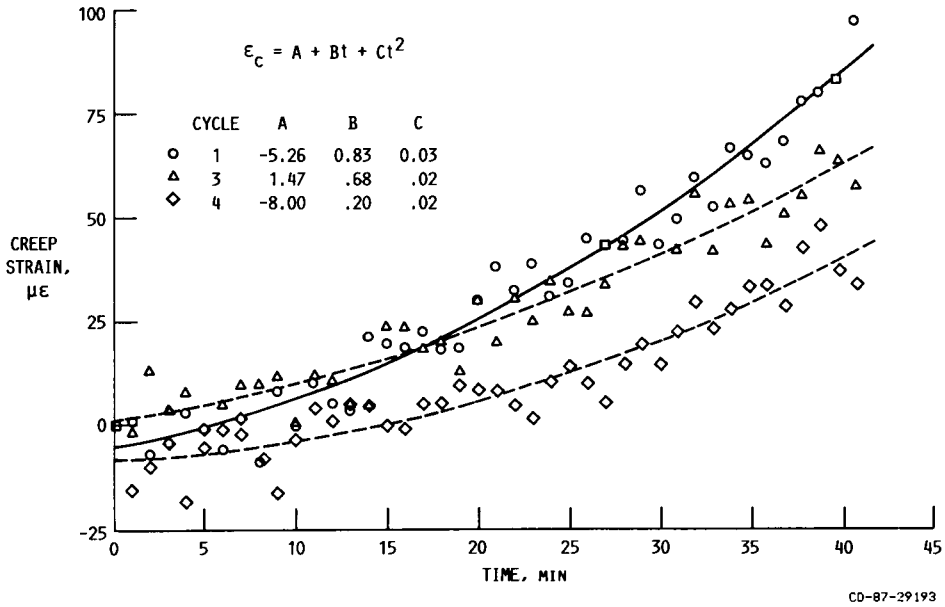


Figure 16